

# A 2-Pyrazoline-Functionalized Zinc Complex: Available N–Ag<sup>I</sup> Interaction Modulating Its Fluorescence Properties

Hui-hui Zhang,<sup>[a]</sup> Wei Dou,<sup>[a]</sup> Wei-sheng Liu,<sup>\*,[a,b]</sup> Xiao-liang Tang,<sup>[a]</sup> and Wen-wu Qin<sup>[a]</sup>

**Keywords:** Fluorescent probes / Silver / N ligands / Zinc / Supramolecular chemistry

A readily available fluorescent sensor [Zn(1-phenyl-3-methyl-5-hydroxy-4-pyrazolyl phenyl ketone benzoyl hydrazone)<sub>2</sub>] (Zn-PMPB) with simple and conformationally adaptable receptors for silver cation has been designed. The central Zn<sup>2+</sup> ion and ligands in the complex have a synergistic effect on binding interactions with the Ag<sup>+</sup> ion. Zn-PMPB was characterized in detail by various spectroscopic techniques and single-crystal X-ray diffraction. Its photochemical properties for detecting the Ag<sup>+</sup> ion in HEPES buffered

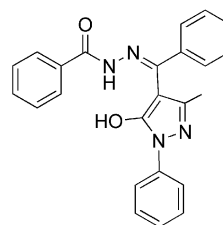
(10 mM, pH 7.1) MeOH/H<sub>2</sub>O (4:6) solution are described. This fluorescent sensor has a negligible quantum yield (0.0011) due to deactivation of solvent hydrogen bonding, whereas a significant increase in fluorescence is observed upon complexation with Ag<sup>+</sup>. NMR titration and UV/Vis spectroscopy suggest that the Ag<sup>+</sup> ions bind to the N2 atom in the pyrazoline group in Zn-PMPB, which facilitates the intramolecular charge transfer emission of pyrazoline.

## Introduction

Pyrazoline has been applied as a fluorophore widely<sup>[1]</sup> with high quantum yields. In addition, compounds with this skeleton have been utilized as fluorescence probes in some elaborated chemosensors because their emission maximum wavelength and quantum yield are sensitive to solvent dipolarity ( $\pi^*$ ) and hydrogen-bond acidity ( $\alpha$ ).<sup>[2]</sup> On the other hand, some fluorescent triarylpyrazolines analogues such as 3-(2-pyridyl)<sup>[3]</sup> themselves can serve as N,N-type bidentate ligands for metal ions. In these intrinsic fluorescent ligands, the metal ion binding affects intramolecular charge transfer and consequently induces both absorbance and emission spectral changes. The foregoing behavior was also applicable to the sensing of metal ions.<sup>[4]</sup>

Pyrazolone, as a prominent structural motif, is found in numerous active compounds. Due to its easy preparation and its rich biological activity of broad-spectrum antibacterial action, antitumor, antiseptic,<sup>[5]</sup> pyrazolone and its complexes have received considerable attention in coordination chemistry and medicinal chemistry. 4-Acylpyrazolones can form a variety of Schiff bases and are reported to be superior reagents in biological, clinical, and analytical applications.<sup>[6]</sup> Meanwhile, compounds containing hydrazide and

acylhydrazone moieties and their complexes also possess biological activities, especially as potential inhibitors for many enzymes.<sup>[7]</sup> However, to the best of our knowledge, no example of the modulation of the fluorescence properties of a pyrazolone Schiff base complex by metal ions has been reported. In this study, a new rigid pyrazole-containing zinc Schiff base complex (Zn-PMPB) with high preorganization and stability<sup>[8]</sup> (Scheme 1) was designed, and its absorption and fluorescence properties modulated by metal ions were investigated.



Scheme 1. Illustration of ligand HPMPB.

## Results and Discussion

### Synthesis and Characterization

As shown in Figure 1, Zn-PMPB exhibits a mononuclear structure with the Zn<sup>2+</sup> center coordinated by two imine nitrogen atoms, two benzoyl oxygen atoms, and two pyrazolone oxygen atoms in a distorted octahedral geometry. As shown in the structure of Zn-PMPB (Supporting Information, Table S1), the C7–O1 and C30–O3 bond lengths are 1.272(3) and 1.268(3) Å, respectively, indicating that pyr-

[a] College of Chemistry and Chemical Engineering, Key Laboratory of Nonferrous Metals Chemistry and Resources Utilization of Gansu Province and State Key Laboratory of Applied Organic Chemistry, Lanzhou University, Lanzhou 730000, China  
Fax: +86-931-8912582  
E-mail: liuws@lzu.edu.cn

[b] State Key Laboratory of Coordination Chemistry, Nanjing University, Nanjing 210093, China

Supporting information for this article is available on the WWW under <http://dx.doi.org/10.1002/ejic.201001083>.

azolone is partly in the enol form. The C17–O2 and C40–O4 distances are 1.233(4) and 1.239(4) Å, respectively, and are similar to the value of 1.234 Å typical of amides of carboxylic acids and appreciably longer than the mean of 1.192 Å found for C=O bonds in ketones. The C17–N4 and C40–N8 distances in Zn-PMPB [1.348(4) and 1.347(4) Å, respectively] are shorter than the database mean<sup>[9]</sup> of 1.376 Å for C<sub>sp<sup>2</sup></sub>–N bonds in imidazoles, which also have some multiple-bond character. These changes show that the amide moiety in the ligand was partly in the enol form.

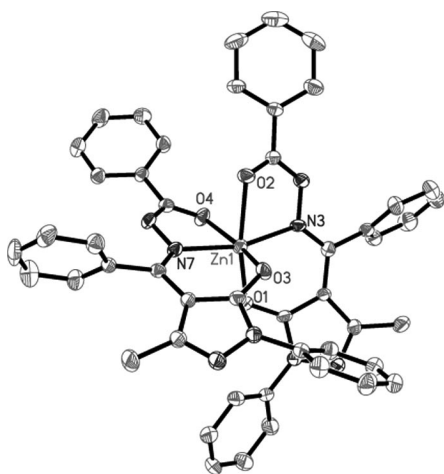


Figure 1. ORTEP diagram (30% probability ellipsoids) showing the coordination sphere of Zn-PMPB with atom labeling scheme; H atoms attached to C atoms and water molecule in the crystal cell are omitted for clarity.

Notably, significant intermolecular hydrogen-bonding interactions exist between two molecules (Figure 2). Two adjacent molecules are held together into 1D supramolecular chains through hydrogen bonding between a water molecule and the pyrazoline nitrogen atoms and between a water molecule and the amide nitrogen atoms. It is remarkable that these intermolecular hydrogen bonds are the most important factors influencing the torsion of the 1-phenyl moiety of pyrazoline and the phenyl group of benzoyl hydrazone.

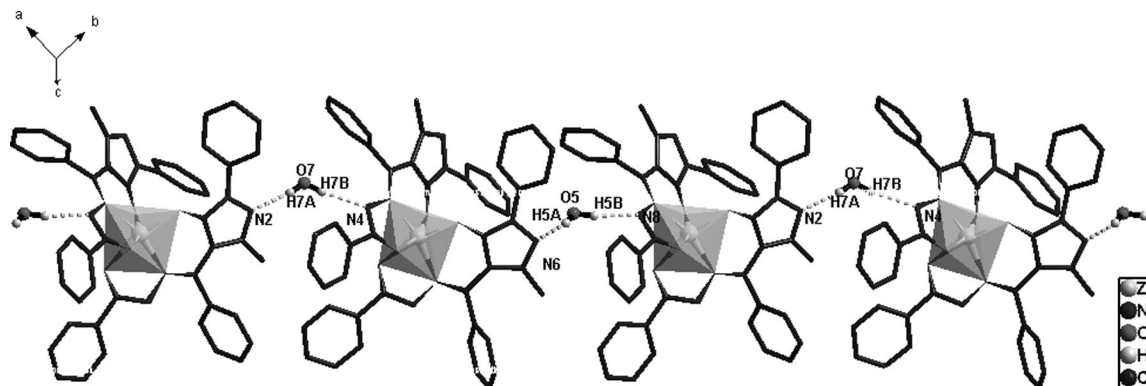


Figure 2. 1D supramolecular chains of Zn-PMPB constructed through hydrogen bonds, which are indicated by dashed lines.

## Fluorescence Properties

In HEPES-buffered (10 mM, pH 7.1) MeOH/H<sub>2</sub>O (4:6) solution, the fluorescence spectrum (Figure 3) of Zn-PMPB showed weak emission bands at 440 and 467 nm (excitation 410 nm), which originated from  $\pi$ – $\pi^*$  of ligand and intra-molecular charge transfer (ICT) emission, respectively. Then the influence of metal ions on the fluorescence spectra of Zn-PMPB was investigated (Figure 3). Ca<sup>2+</sup>, Mg<sup>2+</sup>, Na<sup>+</sup>, and K<sup>+</sup>, did not cause an enhancement in the fluorescence. Other transition metal ions including Mn<sup>2+</sup>, Pb<sup>2+</sup>, Cd<sup>2+</sup>, Co<sup>2+</sup>, Zn<sup>2+</sup>, Ni<sup>2+</sup>, and Cr<sup>3+</sup> had no effect on the fluorescence spectrum of Zn-PMPB. Cu<sup>2+</sup>, Cu<sup>+</sup>, and Hg<sup>2+</sup> obviously quenched its fluorescence. However, Ag<sup>+</sup> exhibited completely different behavior (Figure 4). Upon addition of small amounts of Ag<sup>+</sup>, only the peak at 467 nm increased. Upon addition of 1 equivalent of Ag<sup>+</sup> ions (*c* = 50  $\mu$ M), the fluorescence intensity of Zn-PMPB showed a ca. fivefold increase, accompanied by an increase in the quantum yield from 0.11 to 5.1%. Compared with the fluorescence spectra in the absence of Ag<sup>+</sup> ions, the emission band became broader and redshifted, which may be the result of increased dipolarity of the excited state. It is well known that the coordination sphere of Ag<sup>+</sup> is very flexible and that it can adopt coordination numbers between two and six and various geometries from linear through trigonal to tetrahedral, trigonal pyramidal, and octahedral.<sup>[10]</sup> Most important of all, Ag<sup>+</sup> ions always adopt unique linear coordination geometries when coordinated with N-heterocyclic ligands. There are many examples reported on silver supramolecular architectures by using pyrazoline as an electron donor.<sup>[11]</sup> Thus, Ag<sup>+</sup> may be bound with the N2 atom on the pyrazoline, which serves as an exodentate ligand on the basis of its unique linear *s*–*d* hybrid orbitals.<sup>[12]</sup> Therefore, the binding of the N2 atom with the Ag<sup>+</sup> ion increases the dipolarity of the  $\pi^*$  orbital, inhibits the deactivation of solvent hydrogen bonding, and facilitates ICT in C1–N1–N2–C3 when excited.<sup>[1]</sup> To confirm the important role of Zn<sup>2+</sup> ions in the sensor, the fluorescence spectra (Supporting Information, Figure S1) of HPMPB in the presence of Ag<sup>+</sup> ions were measured under the same conditions, which did not exhibit obvious changes. Thus, the binding of Zn<sup>2+</sup> ions

with the PMPB ligand improves the selective recognition ability of the ligand to  $\text{Ag}^+$  due to increased rigidity and high preorganization.

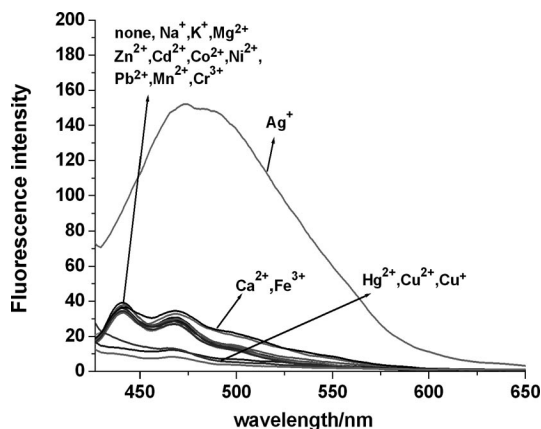


Figure 3. Fluorescence spectra of Zn-PMPB ( $50 \mu\text{M}$ ) and fluorescence spectra of Zn-PMPB ( $50 \mu\text{M}$ ) in the presence of 5 equiv. of different metal ions in HEPES-buffered (10 mM, pH 7.1) MeOH/ $\text{H}_2\text{O}$  (4:6) solution with excitation at 410 nm.

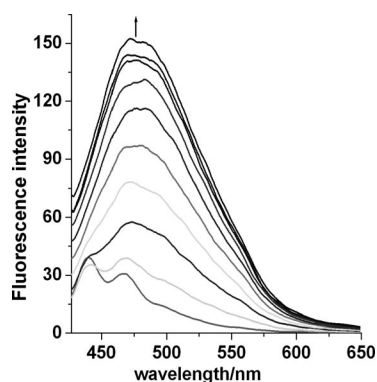


Figure 4. Fluorescent titrations of Zn-PMPB ( $50 \mu\text{M}$ ) in HEPES-buffered (10 mM, pH 7.1) MeOH/ $\text{H}_2\text{O}$  (4:6) upon addition of  $\text{Ag}^+$  in methanol.

To further explore the specific binding between Zn-PMPB and  $\text{Ag}^+$ , competition experiments were also performed (Supporting Information, Figure S2). Alkali metal and alkali earth metal ions hardly interfere with  $\text{Ag}^+$  binding. However, transition-metal ions interfered with  $\text{Ag}^+$  binding.

The Job method monitored by fluorescence intensities was applied to examine the stoichiometry of the Zn-PMPB/ $\text{Ag}^+$  complex, indicating a 1:1 stoichiometry of Zn-PMPB to  $\text{Ag}^+$  in the complex (Figure 5). Thus, the association constant ( $K_a = 5 \times 10^5 \text{ M}^{-1}$ ) for  $\text{Ag}^+$  was determined by plotting the fluorescence intensity ( $F - F_0$ ) against  $[\text{Ag}^+]$  and fitting these data<sup>[13]</sup> (Supporting Information, Figure S13).

Silver-bound forms of Zn-PMPB have stable fluorescence at biological pH (Figure 6). The fluorescence of Zn-PMPB in the absence of  $\text{Ag}^+$  did not change over a wide

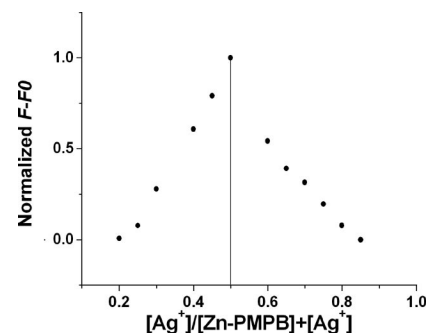


Figure 5. Job plot for determining the stoichiometry of Zn-PMPB and  $\text{Ag}^+$  in HEPES-buffered (10 mM, pH 7.1) MeOH/ $\text{H}_2\text{O}$  (4:6) solution. The sum of the concentration of Zn-PMPB and  $\text{Ag}^+$  is  $50 \mu\text{M}$ .

range of pH values (from 2 to 12). The fluorescence intensity of Zn-PMPB in the presence of  $\text{Ag}^+$  did not change below pH 8 and decreased as the pH value increased due to the competition of hydrolysis.

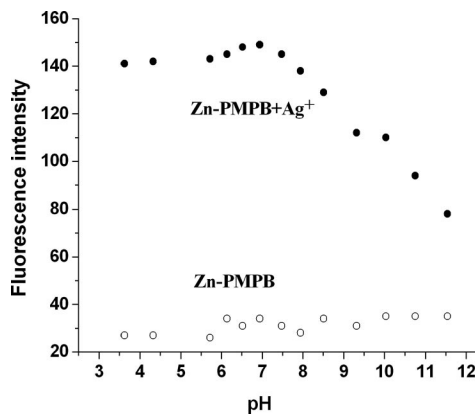


Figure 6. Effect of pH on the emission intensity of Zn-PMPB and its  $\text{Ag}^+$  complex at 474 nm:  $50 \mu\text{M}$  Zn-PMPB +  $50 \mu\text{M}$   $\text{Ag}^+$  (closed circle) and  $50 \mu\text{M}$  Zn-PMPB (open circle).

### Absorption Properties

To examine the optical properties of Zn-PMPB with metal ions, the tested metal ions  $\text{Na}^+$ ,  $\text{K}^+$ ,  $\text{Ca}^{2+}$ ,  $\text{Mg}^{2+}$ ,  $\text{Cr}^{3+}$ ,  $\text{Mn}^{2+}$ ,  $\text{Co}^{2+}$ ,  $\text{Ni}^{2+}$ ,  $\text{Fe}^{3+}$ ,  $\text{Cu}^{2+}$ ,  $\text{Ag}^+$ ,  $\text{Zn}^{2+}$ ,  $\text{Cd}^{2+}$ ,  $\text{Hg}^{2+}$ , and  $\text{Pb}^{2+}$  ( $50 \mu\text{M}$ ) were added to the solution of Zn-PMPB ( $50 \mu\text{M}$ ). The  $\text{Ag}^+$  ion induced fair changes in the absorption spectra (Figure 7): the band around 300 nm assigned to C=N transition<sup>[14]</sup> increased, which indicates that the extent of enolization of the amide moiety increased after  $\text{Ag}^+$  ion binding with N2. Meanwhile, the absorption of the pyrazolone ring was broadened at longer wavelength, which implies that the dipolarity and conjugate area of the pyrazolone ring were enhanced after  $\text{Ag}^+$  ion binding with the N2 atom. The replacement of  $\text{Zn}^{2+}$  by  $\text{Ag}^+$  can be ruled out due to the remarkably different stabilities of Zn-PMPB and  $\text{Ag}^+$ -PMPB in solution (Supporting Information, Figures S3 and S4). However,  $\text{Cu}^{2+}$ ,  $\text{Fe}^{3+}$ , and  $\text{Hg}^{2+}$  ions in-

duced significant changes in the absorption spectra (Supporting Information, Figures S5–S7). The control spectra for Cu-PMPB, Fe-PMPB, and Hg-PMPB indicated that these ions replaced the  $Zn^{2+}$  ions and coordinated with PMPB (Supporting Information, Figures S8–S10). With respect to other metal ions, such as  $Na^+$ ,  $K^+$ ,  $Ca^{2+}$ ,  $Mg^{2+}$ ,  $Cr^{3+}$ ,  $Mn^{2+}$ ,  $Co^{2+}$ ,  $Ni^{2+}$ ,  $Zn^{2+}$ ,  $Cd^{2+}$ , and  $Pb^{2+}$ , they did not cause any obvious spectral changes (Supporting Information, Figure S11).

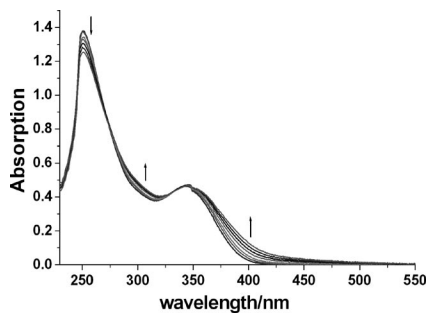


Figure 7. UV/Vis absorption spectra of Zn-PMPB (50  $\mu M$ ) in HEPES-buffered (10 mM, pH 7.1) MeOH/H<sub>2</sub>O (4:6) solution upon the addition of  $Ag^+$ . The final total concentration of  $Ag^+$  is 50  $\mu M$ .

### Binding Mode of the Zn-PMPB/ $Ag^+$ Complex

To give a clear receptor– $Ag^+$  complexation structure, we recorded the  $^1H$  NMR spectra (Figure 8) of Zn-PMPB in the presence of different concentrations of  $Ag^+$  ions. Because of the poor solubility of the Zn-PMPB/ $Ag^+$  complex,  $^1H$  NMR titration experiments were conducted in DMSO solvent. The signal of the protons on the 3-methyl group splits into three peaks due to the different electron distributions in the two ligands. After the addition of 0.5 equiv. of  $AgSO_3CF_3$  in DMSO to Zn-PMPB in DMSO, these peaks were shifted upfield significantly. This shift approximately reaches its limit after the addition of 1 equiv. of  $Ag^+$  ions, consistent with Job's plot analysis by using fluorescence data, which indicates a 1:1 Zn-PMPB/ $Ag^+$  coordination mode. The upfield shift of the 3-methyl peaks suggested an increase in the charge density due to the decrease in the dihedral angle between the 1-phenyl ring and the pyrazolyl ring after binding of the  $Ag^+$  ions. However, the peaks were blunt upon the addition of 2 equiv. of  $Ag^+$  ions, which may be due to the formation of oligomeric products such as  $Ag/Zn-PMPB/Ag/Zn-PMPB/Ag$  because the concentrations of  $Ag^+$  and Zn-PMPB were high in the NMR titration experiment. Although attempts to grow good quality single crystals of the Zn-PMPB/ $Ag^+$  adduct were not successful, the above results from the  $^1H$  NMR titration experiment hint at possible  $Ag^+$  coordination with Zn-PMPB. In addition, a peak cluster at  $m/z = 964.5$  corresponding to a formula of  $[Zn-PMPB + Ag^+]^+$  (calcd.  $m/z = 964.2$ ) was observed in the MALDI-TOF mass spectrum (Supporting Information, Figure S12).

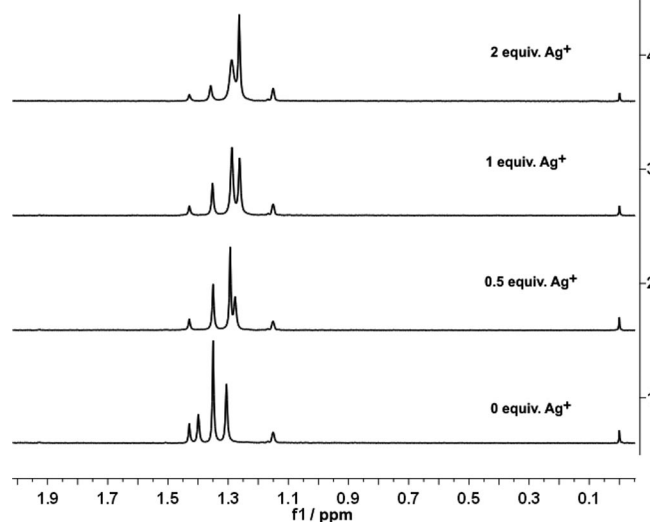


Figure 8.  $^1H$  NMR spectra of Zn-PMPB (in DMSO, 3 mm) in the presence of different concentrations of  $Ag^+$  ions.

### Conclusions

In summary, we have designed and synthesized a pyrazoline-functionalized zinc complex (Zn-PMPB) with simple and conformationally adaptable receptors that show fluorescence enhancement on the basis of available pyrazolyl N– $Ag^+$  ion interaction. The remarkable modulation signal based on the photochemical properties of the complex suggests that the use of a metal complex rather than organic dyes as a luminescent probe for cations could effectively construct the higher level recognition system by synergistic effects between the central ion and the ligands. We are actively exploring the preparation of such cooperative sensors.

### Experimental Section

**General Information and Materials:**  $^1H$  NMR and  $^{13}C$  NMR spectra were measured with a Varian Mercury plus 300M spectrometer in  $CDCl_3$  solution with TMS as an internal standard. NMR titration was conducted with a Bruker-400 spectrometer in DMSO solution with TMS as an internal standard. C, N, and H analyses were performed with an Elementar Vario EL. Melting points were determined with a Kofler apparatus. IR spectra were recorded with a Nicolet FT-170SX instrument by using KBr discs in the 400–4000  $cm^{-1}$  region. ESI-TOF mass spectra were measured with a Mariner MS spectrometer. MALDI-TOF mass spectra were measured with a BIFLEX III (Bruker Daltonics Inc.) MS spectrometer. UV/Vis spectra were obtained by using a Varian UV-Cary 100 spectrophotometer. Fluorescence measurements were made with a Hitachi F-4500 spectrophotometer at room temperature. All pH measurements were made with a pH-10C digital pH meter. All reagents and chemicals were received from commercial sources and used without further purification. Deionized water was used. HEPES buffer solutions (10 mM, pH 7.1) were prepared in MeOH/H<sub>2</sub>O (4:6).

**1-Phenyl-3-methyl-5-hydroxy-4-pyrazolyl Phenyl Ketone Benzoyl Hydrazone (HPMPB) and Complex Zn-PMPB/HPMPB:** Prepared by condensation of the corresponding pyrazolone with benzoyl hydrazine in methanol at reflux according to known literature pro-

cedures.<sup>[15]</sup> Yield 80%. Yellow prisms, m.p. 199.1–200.1 °C. C<sub>24</sub>H<sub>20</sub>N<sub>4</sub>O<sub>2</sub> (396.44): calcd. C 72.70, H 5.08, N 14.13; found C 72.76, H 5.32, N 14.44. <sup>1</sup>H NMR (300 MHz, CDCl<sub>3</sub>, Me<sub>4</sub>Si): δ = 1.541 (s, 3 H), 7.335 (m, 1 H), 7.401–7.601 (m, 8 H) 7.626 (m, 3 H), 7.96 (d, *J* = 7.8 Hz, 2 H), 8.02 (d, *J* = 8.1 Hz, 2 H) ppm. <sup>13</sup>C NMR (75 MHz, CDCl<sub>3</sub>): δ = 163.6, 163.4, 154.3, 149.2, 138.8, 132.7, 132.5, 132.3, 130.6, 129.9, 129.3, 128.8, 128.6, 127.5, 125.1, 120.2, 99.0, 16.2 ppm. ESI-MS: *m/z* = 397.2 [M + H]<sup>+</sup>.

**Zn-PMPB:** To a solution of HPMPB (39.6 mg, 0.1 mmol) in methanol (10 mL) was added an equimolar amount of LiOH, followed by Zn(NO<sub>3</sub>)<sub>2</sub>·6H<sub>2</sub>O (14.7 mg, 0.05 mmol). A precipitate was produced immediately, and the mixture was stirred for 3 h (yield 34.6 mg, 81%). The precipitate was dissolved in small amount of DMF and then methanol was added. The dilute solution was evaporated at room temperature to give yellow crystals of Zn-PMPB suitable for X-ray crystal analysis. C<sub>48</sub>H<sub>38</sub>N<sub>8</sub>O<sub>4</sub>Zn (855.26): calcd. C 67.33, H 4.47, N 13.09; found C 67.21, H 4.61, N 12.94. FTIR (KBr):  $\tilde{\nu}$  = 1594 (CO), 1554 (CN), 1483 (CN) cm<sup>-1</sup>. <sup>1</sup>H NMR (400 MHz, CDCl<sub>3</sub>, Me<sub>4</sub>Si): δ = 8.12 (d, *J* = 7.8 Hz, 2 H), 8.07 (d, *J* = 7.5 Hz, 2 H), 7.63–7.53 (m, 3 H), 7.47–7.35 (m, 4 H), 7.25–7.21 (m, 4 H), 1.57 (s, 3 H) ppm. <sup>13</sup>C NMR (DMSO): δ = 165.9, 163, 162, 147.4, 139.4, 133.1, 132.5, 131.0, 130.1, 129.5, 129.1, 128.5, 128.3, 127.7, 127.3, 124.0, 119.7, 118.4, 97.1, 15.5 ppm. ESI-MS: *m/z* = 856.2 [M + H]<sup>+</sup>.

**Fluorescence and Absorption Spectrophotometry:** Fluorometric titration method, similar to that of UV/Vis titration, was carried out with a solution containing Zn-PMPB (0.05 mM) in MeOH/H<sub>2</sub>O (4:6) with a little DMF added for dissolution. The excitation and emission slit widths were 5 nm. Na<sup>+</sup>, Mg<sup>2+</sup>, Ca<sup>2+</sup>, Mn<sup>2+</sup>, Co<sup>2+</sup>, Ni<sup>2+</sup>, Cd<sup>2+</sup>, Fe<sup>3+</sup>, Pb<sup>2+</sup>, Cu<sup>2+</sup>, Zn<sup>2+</sup>, Hg<sup>2+</sup>, and Ag<sup>+</sup> were prepared from perchlorate or trifluoromethanesulfonic salts. In a typical titration, a volume of 2 mL was used for all measurements and 5 μL aliquots of 8 mM metal ion solution in methanol were added to a solution of 50 μM receptor solution. The emission spectrum was recorded after each solution reacted for 0.5 min. The overall volume change for each experiment did not exceed ca. 5%. Quantum yields were determined by an absolute method using an integrating sphere on FLS920 of Edinburgh instrument. All spectra were recorded at 20 °C. All measurements were conducted at least in triplicate.

**CAUTION:** Although problems were not encountered during the course of this work, attention is drawn to the potentially explosive nature of perchlorates.

**Crystallography:** Single-crystal X-ray diffraction measurements were carried out with a Bruker SMART 1000 CCD diffractometer operating at 50 kV and 30 mA by using Mo-*K*<sub>α</sub> radiation ( $\lambda$  = 0.71073 Å). Each selected crystal was mounted inside a Lindemann glass capillary for data collection by using the SMART and SAINT software. An empirical absorption correction was applied by using the SADABS program. The structure was solved by direct methods and refined by full-matrix least-squares on *F*<sup>2</sup> by using the SHELXTL-97 program package.<sup>[16]</sup> All non-hydrogen atoms were subjected to anisotropic refinement and all hydrogen atoms except those of lattice water molecules were added in idealized positions and refined isotropically. Crystal data and details of the refinement for Zn-PMPB are summarized in Table 1, and representative bond lengths [Å] and angles [°] are presented in the Supporting Information (Table S1). CCDC-707731 (for Zn-PMPB) contains the supplementary crystallographic data for this paper. These data can be obtained free of charge from The Cambridge Crystallographic Data Centre via www.ccdc.cam.ac.uk/data\_request/cif.

Table 1. Crystal data and structure refinement parameters for Zn-PMPB.

	C <sub>48</sub> H <sub>38</sub> N <sub>8</sub> O <sub>4</sub> Zn·3H <sub>2</sub> O
<i>M</i> <sub>r</sub>	910.30
Crystal system	monoclinic
Space group	<i>P</i> 2 <sub>1</sub> / <i>c</i>
<i>a</i> [Å]	15.6931(16)
<i>b</i> [Å]	19.118(3)
<i>c</i> [Å]	17.0355(14)
$\alpha$ [°]	90.00
$\beta$ [°]	117.682(7)
$\gamma$ [°]	90.00
<i>V</i> [Å <sup>3</sup> ]	4526.0(8)
Crystal size [mm]	0.35 × 0.14 × 0.10
<i>Z</i>	4
<i>D</i> <sub>calcd.</sub> [g cm <sup>-3</sup> ]	1.336
<i>T</i> [K]	293(2)
$\theta$ range for data collection [°]	1.5–25.0
$\mu$ (Mo- <i>K</i> <sub>α</sub> ) [mm <sup>-1</sup> ]	0.603
<i>F</i> (000)	1896
Data collected, unique	22041, 7955
<i>R</i> <sub>int</sub>	0.074
<i>R</i> <sub>1</sub> , <i>wR</i> <sub>2</sub> [ <i>I</i> > 2σ( <i>I</i> )]	0.056, 0.060
<i>R</i> <sub>1</sub> , <i>wR</i> <sub>2</sub> (all data)	0.1147, 0.0685
Parameter	579
Goodness of fit on <i>F</i> <sup>2</sup>	0.944
$\Delta$ (max, min) [e Å <sup>-3</sup> ]	–0.32, 0.45

**Supporting Information** (see footnote on the first page of this article): Characterization data for the compounds described; UV/Vis of Zn-PMPB with various metal ions addition; UV/Vis spectra of HPMPB with Ag<sup>+</sup>, Cu<sup>2+</sup>, Hg<sup>2+</sup>, Fe<sup>3+</sup>; and determination of association constants by fluorescence spectroscopy.

## Acknowledgments

The work was supported by the National Nature Science Foundation of China (Grant Nos. 20771048, 20931003) and the Fundamental Research Funds for the Central Universities (lzujbky-2009-k06).

- [1] a) A. Wagner, C. W. Schelhammer, J. Schroeder, *Angew. Chem.* **1966**, *78*, 769; *Angew. Chem. Int. Ed. Engl.* **1966**, *5*, 699–704; b) F. Wilkinson, G. P. Kelly, C. Michael, *J. Photochem. Photobiol. A: Chem.* **1990**, *52*, 309–320; c) J. Barbera, K. Clays, R. Gimenez, S. Houbrechts, A. Persoons, J. L. Serrano, *J. Mater. Chem.* **1998**, *8*, 1725–1730; d) D. Xiao, L. Xi, W. Yang, H. Fu, Z. Shuai, Y. Fang, J. Yao, *J. Am. Chem. Soc.* **2003**, *125*, 6740–6745.
- [2] a) R. A. Bissell, A. P. de Silva, H. Q. N. Gunaratne, P. L. M. Lynch, G. E. M. Maguire, C. P. McCoy, K. R. A. Sandanayake, *Top. Curr. Chem.* **1993**, *168*, 223–264; b) A. P. de Silva, H. Q. N. Gunaratne, T. Gunnlaugsson, A. J. Huxley, C. P. McCoy, J. T. Rademacher, T. E. Rice, *Chem. Rev.* **1997**, *97*, 1515–1566; c) M. D. P. de Costa, A. P. de Silva, S. T. Pathirana, *Can. J. Chem.* **1987**, *65*, 1416–1419; d) S. Pramanik, P. Banerjee, A. Sarkar, A. Mukherjee, K. K. Mahalanabis, S. C. Bhattacharya, *Spectrochim. Acta Part A* **2008**, *71*, 1327–1332.
- [3] a) Y. Toi, M. Kawai, K. Isagawa, T. Maruyama, Y. Fushizaki, *Nippon Kagaku Zasshi* **1965**, *86*, 1322–1327; b) Y. Toi, M. Kawai, K. Isagawa, Y. Fushizaki, *Nippon Kagaku Zasshi* **1967**, *88*, 1095–1099; c) L. Szűcs, *Chem. Zvesti* **1969**, *23*, 677–686.
- [4] a) P. F. Wang, N. Onozawa-Komatsuzaki, Y. Himeda, H. Sugihara, H. Arakawa, K. Kasuga, *Tetrahedron Lett.* **2001**, *42*, 9199–9201; b) H.-B. Shi, S.-J. Ji, B. Bian, *Dyes Pigm.* **2007**, *73*, 394–396.

- [5] a) X. H. Wang, D. Z. Jia, Y. J. Liang, S. L. Yan, Y. Ding, L. M. Chen, Z. Shi, M. S. Zeng, G. F. Liu, L. W. Fu, *Cancer Lett.* **2007**, *249*, 256–270; b) Z. Y. Yang, R. D. Yang, F. S. Li, K. B. Yu, *Polyhedron* **2000**, *19*, 2599–2604; c) A. Kimata, H. Nakagawa, R. Ohyama, T. Fukuuchi, S. Ohta, T. Suzuki, N. Miyata, *J. Med. Chem.* **2007**, *50*, 5053–5056; d) D. Costa, A. P. Marques, R. L. Reis, J. L. F. C. Lima, E. Fernandes, *Free Radical Biol. Med.* **2006**, *40*, 632–640.
- [6] a) M. F. Iskander, L. Sayed, A. F. M. Hefny, S. E. Zayan, *J. Inorg. Nucl. Chem.* **1976**, *38*, 2209–2216; b) H. Adams, D. E. Fenton, G. Minardi, E. Mura, M. Angelo, *Inorg. Chem. Commun.* **2000**, *3*, 24–28.
- [7] a) X.-B. Zhao, H. Yu, S.-W. Yu, F. Wang, J. C. Sacchettini, R. S. Magliozzo, *Biochemistry* **2006**, *45*, 4131–4140; b) A. Parenty, X. Moreau, J.-M. Campagne, *Chem. Rev.* **2006**, *106*, 911–939; c) S. Broussy, V. B. Genisson, A. Quemard, B. Meunier, J. Bernadou, *J. Org. Chem.* **2005**, *70*, 10502–10510; d) A. Mai, S. Massa, R. Ragno, I. Cerbara, F. Jesacher, P. Loidl, G. Brosch, *J. Med. Chem.* **2003**, *46*, 512–524.
- [8] S. Choudhary, J. R. Morrow, *Angew. Chem.* **2002**, *114*, 4270; *Angew. Chem. Int. Ed.* **2002**, *41*, 4096–4098.
- [9] G. Orpen, L. Brammer, F. H. Allen, O. Kennard, D. G. Watson, R. Taylor, *International Tables for Crystallography Vol. C* **1992**, 685–791.
- [10] a) F. A. Cotton, G. Wilkinson, *Advanced Inorganic Chemistry*, 5th ed., Wiley, Chichester, **1988**; b) L. Tei, V. Lippolis, A. J. Blake, P. A. Cooke, M. Schröder, *Chem. Commun.* **1998**, 2633–2634.
- [11] a) J. Kang, M. Choi, J. Y. Kwon, E. Y. Lee, J. Yoon, *J. Org. Chem.* **2002**, *67*, 4384–4386; b) X. Q. Lu, F. Bao, Q. Wu, B. S. Kanga, S. W. Ng, *Acta Crystallogr., Sect. E: Struct. Rep. Online* **2004**, *60*, m362–m363; c) R. H. P. Francisco, Y. P. Mascarenhas, J. R. Lechat, W. Clegg, P. J. Cooper, C. J. Lockhart, D. J. Rushton, *Acta Crystallogr., Sect. B: Struct. Sci.* **1979**, *35*, 177–178; d) W. Clegg, P. J. Cooper, J. C. Lockhart, D. J. Rushton, *Acta Crystallogr., Sect. C: Cryst. Struct. Commun.* **1994**, *50*, 383–386; e) D. L. Reger, R. F. Semeniuc, J. D. Elgin, V. Rassolov, M. D. Smith, *Cryst. Growth Des.* **2006**, *6*, 2758–2768; f) M. H. Shu, C. L. Tu, W. D. Xu, H. B. Jin, J. Sun, *Cryst. Growth Des.* **2006**, *6*, 1890–1896; g) H. V. R. Dias, C. S. P. Gamage, J. Keltner, H. V. K. Diyabalanage, I. Omari, Y. Eyobo, N. R. Dias, N. Roehr, L. McKinney, T. Poth, *Inorg. Chem.* **2007**, *46*, 2979–2987.
- [12] a) F. A. Cotton, G. Wilkinson, *Advanced Inorganic Chemistry*, John Wiley & Sons, New York, **1988**, p. 941; b) L. E. Orgel, *J. Chem. Soc.* **1958**, *90*, 4186–4190.
- [13] For details how to calculate the binding stoichiometries and the binding constants, see: a) K. A. Connors, *Binding Constants*, Wiley, New York, **1987**; b) J. Polster, H. Lachmann, *Spectrometric Titrations*, VCH, Weinheim, **1989**.
- [14] F. R. F. Mohammad, M. A. E. Mokhles, M. S. Mohamad, A. E. S. Fathy, I. A. Mohammed, S. E. T. Abdou, *J. Coord. Chem.* **2008**, *61*, 1983–1996.
- [15] S. N. Rao, D. D. Mishra, R. C. Maurya, N. Nageswara Rao, *Polyhedron* **1997**, *16*, 1825–1829.
- [16] G. M. Sheldrick, *SHELXL-97: Program for the Solution of Crystal Structures*, University of Göttingen, Göttingen, Germany, **1997**.

Received: October 12, 2010

Published Online: December 29, 2010